Thermal characterization and microbiology assay of *Annona muricata* L. leaves

Fabrício Havy Dantas de Andrade[1,2] · Rayanne Sales de Araújo Batista[2] · Taynara Batista Lins[2] ·
Felipe Hugo Alencar Fernandes[3] · Deysiane Oliveira Brandão[2] · Rui Oliveira Macedo[1,2] · Fábio Santos de Souza[2] ·
Almir Gonçalves Wanderley[1]

Abstract

Annona muricata L., Annonaceae, popularly known as soursop, has anticancer and antidiabetic pharmacological properties. This work aims the characterization by thermoanalytical technique and determination of antimicrobial activity of different *A. muricata* L. leaves particle sizes. The leaves were dried, knifed, and separated by particle size. Samples were characterized by scanning electron microscopy (SEM) and thermogravimetry (TG) using the Ozawa kinetics model in two atmospheres (nitrogen and synthetic air). The antimicrobial activity and minimum inhibitory concentration of infusions were performed by the broth microdilution method to *Escherichia coli*, *Staphylococcus aureus*, *Pseudomonas aeruginosa*, and *Klebsiella pneumoniae*. SEM analysis suggests heterogeneous distribution in the observed particle sizes. TG curves were able to differentiate the degradation events and the residue contents in the samples analyzed in the nitrogen and synthetic air atmospheres. In nitrogen atmosphere curves, the different particle sizes presented four mass loss events, and residue ranged from 20.90 to 26.80% at the end of the analysis. In synthetic air atmosphere, the different particle sizes presented three mass loss events, and residue ranged from 7.80 to 10.42%. Ozawa model showed reaction order equal to zero for all samples assayed, and the activation energy (E_a) ranged from 121.36 to 135.42 and 115.50 to 141.00 kJ mol^{-1} for the nitrogen and synthetic air atmospheres, respectively. Antibacterial activity was confirmed for all particle sizes, in special to AM4 with *S. aureus*, *E. coli*, and *K. pneumoniae*. These results indicate that leaves from *A. muricata* L. have great potential for a variety of medicinal applications.

Keywords *Annona muricata* L. · Soursop · Thermal characterization · Herbal medicines · Antimicrobial activity

✉ Fabrício Havy Dantas de Andrade
  fabriciohda@gmail.com

1   Postgraduate Program in Pharmaceutical Sciences,
    Department of Pharmaceutical Sciences, Federal University
    of Pernambuco, University City, Artur de Sá Avenue, Recife,
    PE 50740-521, Brazil

2   Unified Laboratories of Pharmaceutical Development and
    Assays, Pharmaceutical Sciences Department, Federal
    University of Paraíba - UFPB, Campus I, University City s/n,
    Castelo Branco III, João Pessoa, PB 58059-900, Brazil

3   Pharmacy Department, FCM, UNIFACISA - University
    Center, Av. Senador Argemiro de Figueiredo, 1901, Itararé,
    Campina Grande, PB 58411-020, Brazil

Introduction

Annona muricata L., Annonaceae, is also known as soursop, graviola, and guanabana. *A. muricata* L. is mainly found in tropical and subtropical regions of the world. The genus Annona comprises more than 70 species, among which *A. muricata* L. is the most widely cultivated [1]. Pharmacological studies have shown activity against cancer cells [2, 3], antimicrobial [4], antiarthritic, antiparasitic [5], hepatoprotective [6], and antidiabetic [7]. Phytochemical studies have revealed a wide variety of secondary metabolites such as alkaloids, polyphenols [8], flavonoids [9], tannins, and acetogenins [10, 11]; annonacin is the ubiquitous acetogenin present in leaves of *A. muricata* L. [12].

The mechanism of the cytotoxicity of acetogenins is mediated, at least partly, by inhibition of the mitochondrial complex I, depletion of ATP levels via the inhibition of ubiquinone-linked NADH oxidase in the plasma membranes of cancerous cells causing apoptosis [11, 13]. Yang [14] studied the cytotoxicity of annonacin in T24 bladder cancer cells. The T24 line was more sensitive in the S phase; there was cell cycle delay in the G1 phase by the activation of p21 independent of p53. It also induced expression of Bax, increased caspase-3 activity and caused apoptotic cell death in T24 cells.

The search for natural products used to treat and/or prevent diseases has increased interest in herbal medicines, and with it, the search for products with effectiveness, low risk, as well as reproducibility and consistent quality has also increased [15].

The distribution of the particle size of the raw material must be considered in the physical characterization of the inputs, aiming at the standardization and quality of the medicines obtained from plant material [16]. Correia et al. [15] proposed the need to develop methodologies to discriminate particle size in powder. The milling process for dried plants is a critical step in the production of intermediates of herbal medicines due to its importance in the role of particle size control [17].

The quality control of synthetic and natural medicines routinely uses analytical techniques such as liquid and gaseous chromatography and spectrophotometry for the identification and quantification of drugs [18]. Thermoanalytical techniques have gained visibility in the quality control of herbal medicines [19] and are used in the characterization of drugs, compatibility studies, purity determination, polymorphs identification, stability evaluation, and development of pharmaceutical formulations of the synthetic drugs [20–23] and were more recently used in the study of plant material and its derivatives, where the TG proved to be a useful tool for differentiating particle sizes from plant drugs [15, 17, 24–27].

Formulations containing *A. muricata* L. are available on the market as nutraceuticals [28], but thermal characterization studies of the plant material and its extracts are not available. Thus, the aim of this work is to characterize by SEM and TG, to determine the kinetic parameters of decomposition, and to determine antimicrobial activity in different particle sizes of the *A. muricata* L. leaves.

Materials and methods

Plant material

The leaves of *A. muricata* L. were collected in the city of Santa Rita, Paraíba, Brazil (7°14′48.0″S/34°58′40.0″W). The voucher specimen was deposited in the Lauro Pires Xavier herbarium at the Federal University of Paraíba (João Pessoa, Paraíba, Brazil) under the number JPB63746. This access was registered in the National System of Genetic Heritage and Associated Traditional Knowledge (SISGEN) under the number A993C08. The leaves were cleaned and sanitized, then dehydrated in an oven with forced air circulation and a controlled temperature of 40 ± 2 °C for 120 h. The dried material was milled using a knife mill (Marconi, Willey), coupled to a 2-mm opening screen. The dried leaf powder (AM0) was submitted to a sieving system, where the powders were selected with the following size bands: (AM0) < 2.000, 0.500 < (AM1) $\geq$ 0.350, 0.250 < (AM2) $\geq$ 0.149, 0.149 < (AM3) $\geq$ 0.074, (AM4) < 0.074 mm.

Scanning electron microscopy

The morphology evaluation of the samples was performed by scanning electron microscopy (SEM) using a microscope (ZEISS®, LEO 1430). The samples were fixed on carbon double-sided tape and metallized with gold for 1.5 min (EMITECH Metallizer, k550x). The photomicrographs were obtained in a chamber with excitation voltage of 15 kV under atmospheric vacuum of 5-10 Torr.

Thermogravimetry

Dynamic thermogravimetric curves were obtained in a thermobalance (Shimadzu®, TGA-50). The apparatus was calibrated with calcium oxalate monohydrate. The experiments were conducted in temperatures ranging from 25 to 800 °C at heating rates (β) of 5, 10, 20, and 40 °C min^{-1}, in two different atmospheres: one inert using nitrogen and the other using synthetic air with flow of 50 and 20 mL min^{-1}, respectively. The sample mass was 4.0 ± 0.1 mg in alumina crucible. The Ozawa model was used to determine the kinetic parameters: reaction order (n), frequency factor (A), and activation energy (E_a). TG data were analyzed using Shimadzu® TA-60ws software.

Determination of antimicrobial activity

Standard strains used included American Type Culture Collection (ATCC) of *Escherichia coli* (ATCC 25922), *Staphylococcus aureus* (ATCC 25923), *Pseudomonas aeruginosa* (ATCC 27853), and *Klebsiella pneumoniae* (ATCC 4352), which were made available by the Oswaldo Cruz Foundation (Fiocruz, RJ).

Screening microbiology

The method was performed as described by Brandão et al. [29] where the inocula were standardized in tubes
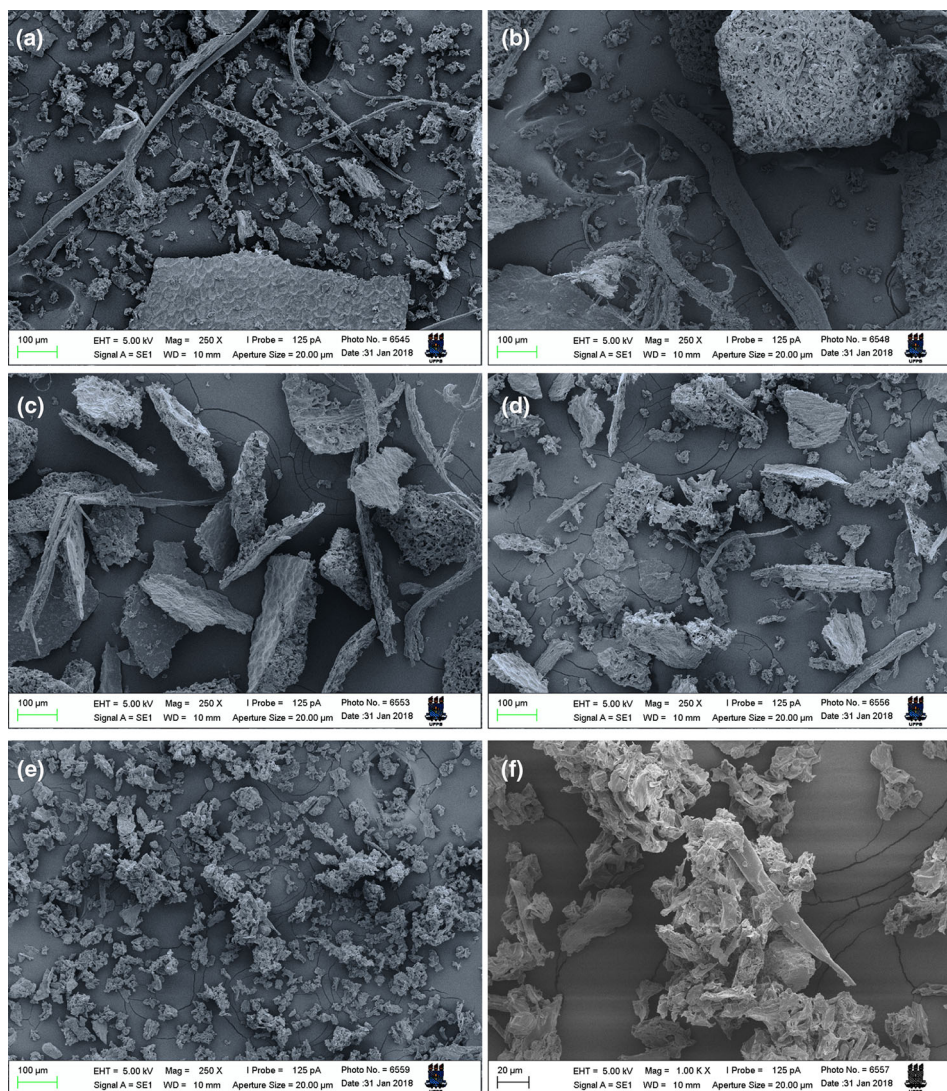
Fig. 1 Photomicrographs of the dried leaf powder of *A. muricata* L. with zoom of 250 times. **a** AM0, **b** AM1, **c** AM2, **d** AM3, **e** AM4 and **f** AM4 with zoom of 1000 times

containing 5 mL of sterile 0.9% saline solution. The suspension was adjusted in a spectrophotometer at 625 nm, at a concentration equivalent to 10^6 UFC. Infusions preparation: 500 mg of the powdered leaves was added to a container with 10 mL of distilled water (98 $\pm$ 2 °C) for 10 min. One hundred microliters of the infusion of the different particle sizes was subjected to serial dilution in Mueller–Hinton broth, thus obtaining the following con-

Table 1 Results of TG analyses of *A. muricata* L. leaves in the nitrogen atmosphere and β 10 °C min^{-1} in different particle sizes

Samples	First Step		Second step		Third step		Fourth step		Residue
	T_{onset}/°C	Δm/%	T_{onset}/°C	Δm/%	T_{onset}/°C	Δm/%	T_{onset}/°C	Δm/%	%
AM0	50.28	5.70	286.57	43.07	375.83	15.37	533.93	11.99	23.97
AM1	39.77	6.21	290.04	43.22	368.27	17.80	565.75	7.51	26.80
AM2	41.35	6.88	279.44	43.25	395.98	17.36	589.93	8.32	22.82
AM3	40.35	7.50	281.13	40.57	363.46	19.80	590.05	8.83	23.31
AM4	40.94	5.74	294.06	43.99	368.28	16.56	570.24	18.89	20.90

Table 2 Results of TG analyses of *A. muricata* L. leaves in the synthetic air atmosphere and β 10 °C min^{-1} in different particle sizes

Samples	First step		Second step		Third step		Residue
	T_{onset}/°C	Δm/%	T_{onset}/°C	Δm/%	T_{onset}/°C	Δm/%	%
AM0	43.39	8.57	290.77	39.05	482.93	40.86	10.42
AM1	39.40	8.11	282.70	39.46	488.13	43.36	7.80
AM2	32.97	7.20	274.46	41.24	479.64	41.22	9.30
AM3	43.26	7.81	274.28	43.47	480.10	39.26	9.00
AM4	36.42	6.70	287.75	43.16	505.55	39.86	10.19

Fig. 2 Dynamic TG curves of AM0 in the nitrogen (NITRO) and synthetic air (AIR) atmospheres and in heating rate of 10 °C min^{-1}
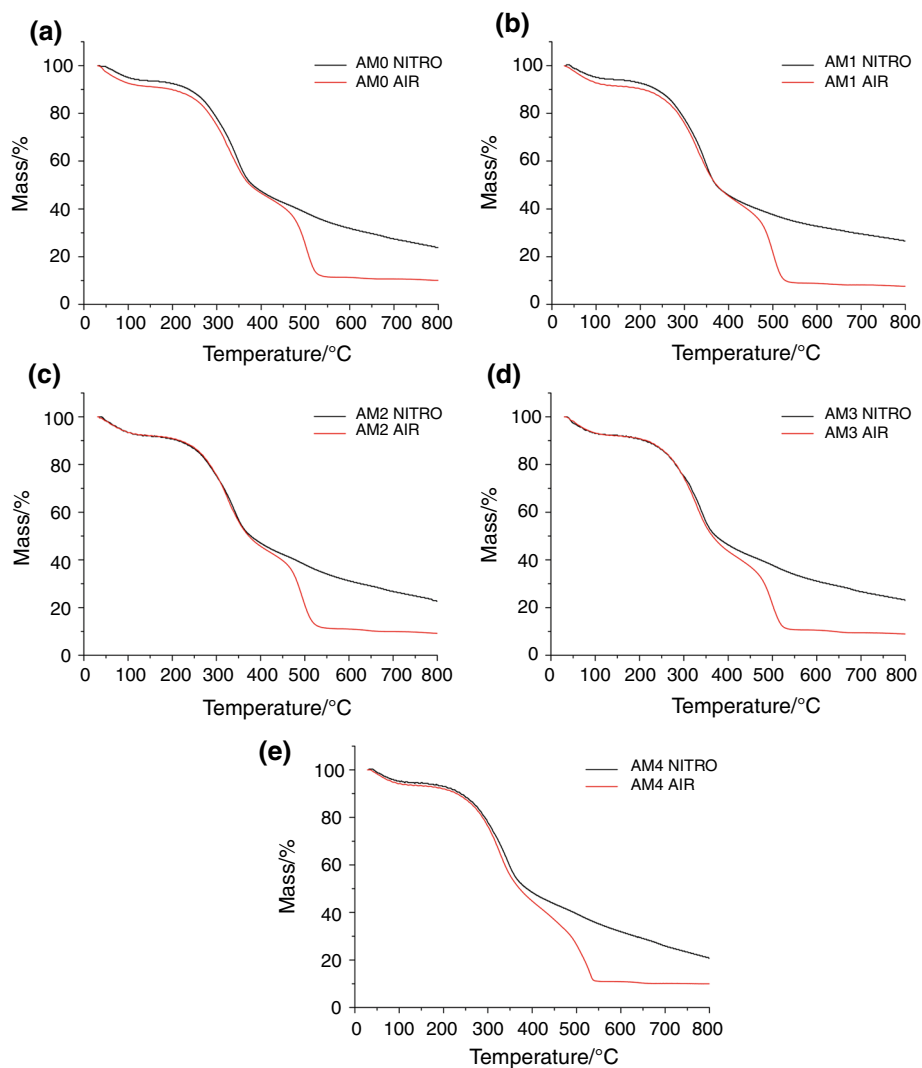
centrations: 25, 12.5, 6.25, 3.12, 1.56, 0.78, 0.39, and 0.195 mg mL^{-1} of each infusion. Ten microliters of each culture of microorganisms was added to the microplate well. Distilled water and gentamicin (80 mg mL^{-1}) were used as negative and positive controls, respectively.

The bacterial growth was indicated by addition of 20 µL of aqueous resazurin (Sigma-Aldrich) 0.01%, with further incubation at 37 ± 1 °C for 2 h. Viable microorganisms reduced the blue dye to a pink color. Thus, MIC was

defined by the lowest concentration without color change of the dye. The assays were performed in triplicate.

Results and discussion

In the development of formulation from medicinal plants, the polarity of the extracting solvent and the particle size may influence the concentration of the secondary

metabolites present in the herbal medicines [16]. Quality control is vital to the safety and quality of herbal medicines; however, the quality of standardization is more difficult because of the lack of interest in the study in the development stage [27].

Photomicrographs of dried leaf powder showed heterogeneous distribution in the observed particle sizes (Fig. 1), with improvement in homogeneous with the reduction in the mean diameter of the samples, and AM4 showed a tendency to agglutination, as shown in Fig. 1f.

We chose to describe the thermal events only for sample AM0, because the other samples with different particle sizes in the same atmosphere conditions and heating rate showed only differences in the values of mass loss and residue. These data are shown in Tables 1 and 2.

Figure 2 shows the TG curves of the samples in the nitrogen and synthetic air atmospheres and β of 10 °C min^{-1}. In the nitrogen atmosphere, AM0 showed four mass loss steps. The first step occurred between 39.77 and 122.80 °C (T_{start} and T_{end}) with mass loss (Δm) 5.70% and can be attributed to the loss of volatiles and water. The second step occurred between 122.80 and 375.83 °C with Δm 43.07%, and the third step occurred between 375.83 and 533.93 °C with Δm 15.37%. The second and third steps represent the degradations of the set of macro- and microconstituents of the samples [24, 25]. The fourth step occurred between 533.93 and 799.57 °C with Δm 11.99%, resulting in residue at the end of the analysis of 23.97%, where the last step is characterized with slow and progressive mass loss resulting in a residue at the end of the analysis of more than 20%. These results are similar to those found by Fernandes et al. [30] for *Spondias dulcis* Parkinson.

In the nitrogen atmosphere, the samples in different particle sizes presented four mass loss steps (Table 1); the second step presented the largest mass loss in this atmosphere, being chosen for the studies of thermal kinetics; the samples AM4 and AM3 presented highest loss of mass in the second and third steps, respectively; and the samples with the largest particle size AM0 (23.97%) and AM1 (26.80%) presented highest residue at the end of the analysis, showing that the heat transfer rate and degradation may have been influenced by the particle size in the nitrogen atmosphere.

In the synthetic air atmosphere, AM0 showed three mass loss steps. The first step occurred between 34.31 and 143.50 °C with mass loss (Δm) 8.57% and can be attributed to the loss of volatiles and water. The second step occurred between 144.43 and 365.15 °C with Δm 39.05%, and the third step occurred between 365.15 and 554.94 °C with Δm 40.86%, resulting in residue at the end of the analysis of 10.42%.

In the synthetic air atmosphere, the samples in different particle sizes presented three mass loss steps (Table 2), and AM3 (43.47%) and AM4 (43.16%) presented highest loss of mass in the second step. The residue obtained at the end of the analysis in this atmosphere aligns with that found by the method of total ashes. This finding is correlated with the presence of oxygen in the degradation using both methods. In the synthetic air atmosphere, the TG curves did not show any more mass loss after 550 °C at the β of 10 °C min^{-1}. These results show that TG can be used with precision as a substitute to the classical methods for determining total ashes of plant material using a synthetic air atmosphere. In this study, the inert atmosphere seems to have delayed the degradation of the samples, with the appearance of the fourth step of degradation and greater residue (Table 1 and Fig. 2).

The last step in the TG curves in the studied atmospheres may be related to the cyclization of aromatic groups and formation of elemental carbon, where the appearance of the material at the end of the analysis showed distinct visual characteristics, with black and white coloration for the residues in nitrogen and synthetic air, respectively.

Guimarães et al. [26] used TG to study the plant drug *Poincianella pyramidalis* after grinding and granulometric separation in different atmospheres. The authors observed changes in the appearance of the carbonized material and attributed those changes to a possible incomplete degradation in the inert atmosphere.

The TG curves of samples at different heating rates showed displacement of the degradation event at higher temperatures with the increase in β. In the nitrogen atmosphere, an increase in the mass of residue was observed with increase in β (Fig. 3).

Particle sizes were evaluated in different atmospheres and β using T_{onset}, thermal degradation steps (second and fourth for the nitrogen atmosphere and second and third for the synthetic air atmosphere), and the residue (Table 3).

There were significant differences across the heating rates in the atmospheres in the second degradation step. There were no significant differences for particle sizes, with p value of 0.816 and 0.821 for the nitrogen and synthetic air atmospheres, respectively. There were no differences in the thermal events attributed to degradation of macro- and microconstituents, possibly due to the mass loss that occurred during these events mainly by volatilization or degradation followed by volatilization at high temperatures [31].

For the events related to elemental carbon formation and cyclization of aromatic groups, the third step in the synthetic air atmosphere did not show differences between particle sizes (p value 0.116), but showed differences for β with p value of 0.002. For the fourth step in the nitrogen

Fig. 3 Dynamic TG curves of *A. muricata L.* leaves in the nitrogen (NITRO) and synthetic air (AIR) atmospheres and in different heating rates. **a** AM0 NITRO, **b** AM0 AIR, **c** AM1 NITRO, **d** AM1 AIR, **e** AM2 NITRO, **f** AM2 AIR, **g** AM3 NITRO, **h** AM3 AIR, **i** AM4 NITRO, **j** AM4 AIR
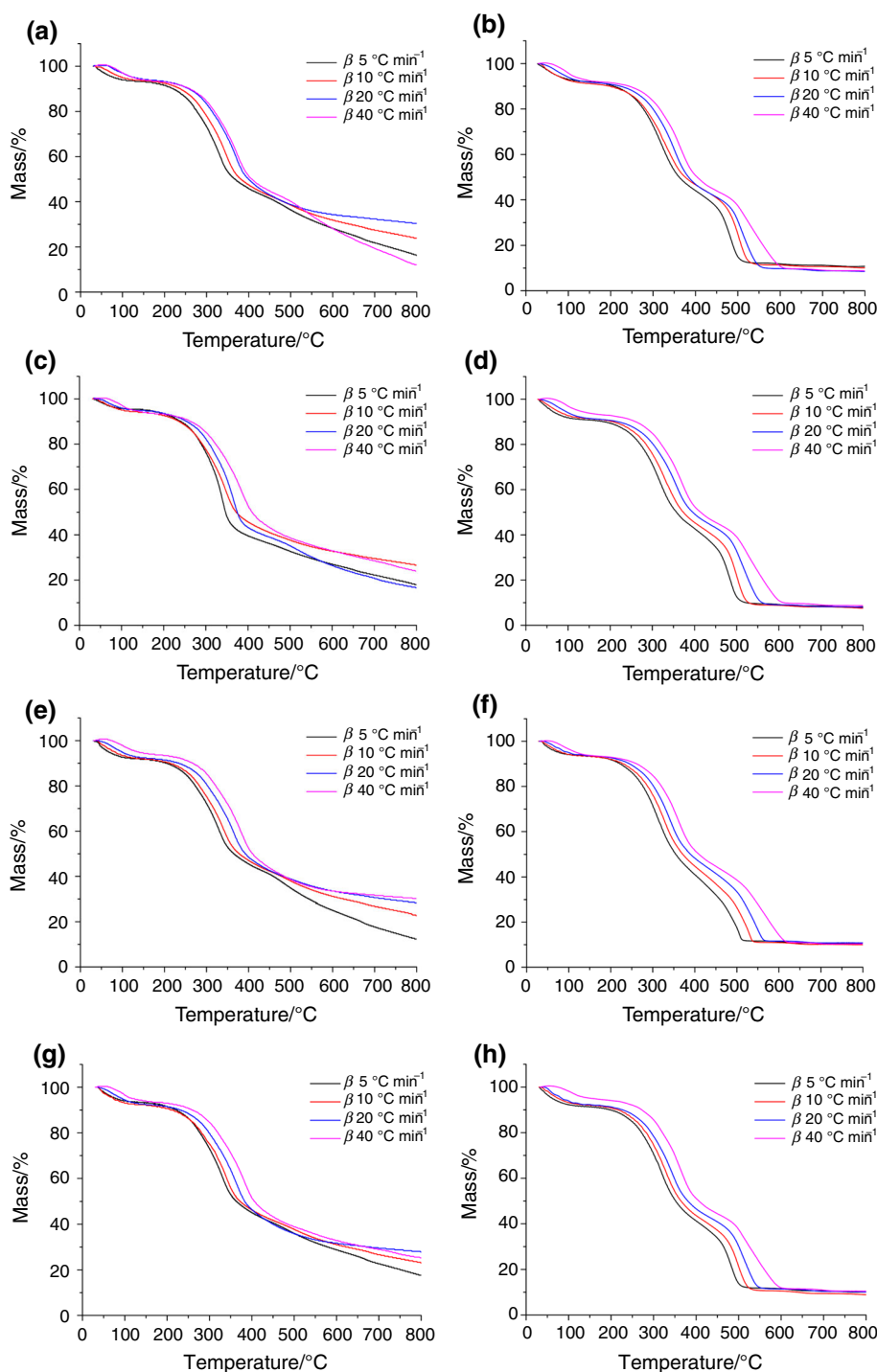
atmosphere, there were no differences between the β (*p* value 0.839), but there were differences in the T_{onset} for particle sizes (*p* value 0.026), with greater influence between the coarse and fine powders (AM0 and AM3).

In the kinetic study of thermal decomposition by dynamic TG, the Ozawa model was applied. In applying this model, it was necessary to obtain four curves under different heating ratios of the different particle sizes. The

decomposition fraction (alpha 0.2) between T_{onset} and T_{endset} of the decomposition event was determined through the derivative of the main event (second event in the atmospheres). The reaction order equalled zero order for all samples. The E_a and A showed different values in the nitrogen and synthetic air atmospheres, as shown in Table 4. The values of E_a obtained were of the following order: AM1 > AM0 > AM3 > AM4 > AM2 and
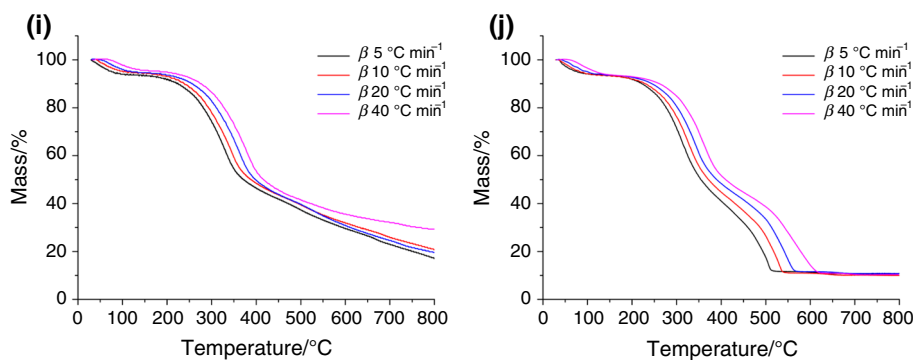
Fig. 3 continued

Table 3 Determination of differences between the samples using *p* value at different heating rates and atmospheres

Events	Nitrogen atmosphere		Synthetic air atmosphere	
	β *p* value	Particle sizes *p* value	β *p* value	Particle sizes *p* value
Second step	0	0.816	0	0.821
Third step	–	–	0.002	0.116
Fourth step	0.839	0.026	–	–
Residue	0.056	0.953	0.676	0.002

β heating rates

Table 5 Antimicrobial activity and MIC determination of soursop leaves tested against microorganisms

Samples	MIC/mg mL^{-1} Microorganisms tested			
	S.a	*E.c*	*P.a*	*K.p*
AM0	3.12	1.56	3.12	3.12
AM1	1.56	1.56	3.12	3.12
AM2	1.56	1.56	1.56	1.56
AM3	0.78	1.56	1.56	0.78
AM4	0.78	0.78	1.56	0.78

MIC minimum inhibitory concentration, *S.a. Staphylococcus aureus*, *E.c. Escherichia coli*, *P.a. Pseudomonas aeruginosa*, *K.p. Klebsiella pneumoniae*

AM4 > AM0 > AM2 > AM3 > AM1 for the nitrogen and synthetic air atmospheres, respectively. In the nitrogen atmosphere, the E_a was higher for AM0 and AM1, whereas in the synthetic air atmosphere, particle size did not influence E_a.

Correia et al. [15] studied different particle sizes of *Tabebuia caraíba* where the decomposition kinetics were of zero order for all of the studied samples, with variations in the degradation process, not showing uniformity in E_a values. The authors concluded that the thermal decomposition was not similar in the plant material in different granulometries, and the E_a values of the samples varied when submitted to the same conditions and data treatment. These results differ from those observed by Brandão et al. [29] studying *Momordica charantia*. These authors

observed reduction in E_a with decreasing particle size of the samples and concluded that the complexity of the plant matrix may induce changes in the kinetic parameters for the different particle sizes, depending on the intrinsic characteristics of the plant material.

The infusions of leaf powders in the different particle sizes were able to inhibit the growth of all gram-positive (*S. aureus*) and gram-negative bacterial strains (*P. aeruginosa*, *E. coli* and *K. pneumoniae*) studied. The improvement of the antimicrobial activity with the reduction in particle size can be attributed to the greater surface area allowing the particles to improve the extraction of active

Table 4 Degradation kinetics using the Ozawa model for the different particle sizes of soursop leaves

Samples	Nitrogen atmosphere		Synthetic air atmosphere	
	E_a/KJ mol^{-1}	A/min^{-1}	E_a/KJ mol^{-1}	A/min^{-1}
AM0	131.16 ± 3.49	9.96E + 09	146.03 ± 5.02	2.67E + 11
AM1	135.79 ± 4.10	7.11E + 10	119.48 ± 3.27	1.32Ev + 09
AM2	117.66 ± 4.18	8.39E + 08	132.21 ± 2.52	1.92E + 10
AM3	126.15 ± 2.60	4.74E + 09	124.10 ± 7.10	4.44E + 09
AM4	125.59 ± 5.43	3.33E + 09	153.85 ± 3.13	1.72E + 12

E_a activation energy, A frequency factor

metabolites with antibiotic action. Table 5 shows the MICs for the different particle sizes.

Radji et al. [32] and Van de Venter et al. [33] reported antimicrobial activity of *A. muricata* L. extract against *Mycobacterium tuberculosis*. Previous studies have shown the activity of other species of the genus Annonaceae, as the ethanol extract of *A. crassiflora* showed activity against *Bordetella bronchiseptica, P. aeruginosa, Rhodococcus equi,* and *S. aureus* [34]; the extracts of *A. ambotay* Aubl. (wood) and *A. cherimolia* Mill (leaves) showed activity against Bacillus subtilis and S. aureus, but hexane extracts from leaves of *A. muricata* L. showed no activity against *B. subtilis, E. coli, Micrococcus luteus, P. aeruginosa* and *S. aureus* [35]. The antimicrobial activity present in aqueous extracts and the presence of activity against gram-positive and gram-negative bacteria can be explained by the influence of the solvent and extraction method on the variety of secondary metabolites extracted [36, 37].

Conclusions

The thermal profile of the leaf powder of *Annona muricata* L. presented third and fourth steps of mass loss with differences in the amount of residue at the end of the analysis, in the synthetic air and nitrogen atmospheres, respectively. The TG made it possible to differentiate the events of thermal degradation and the residual contents in the samples in different sizes of particle. The degradation kinetics using the Ozawa model were determined; the samples showed a reaction order equal to zero, higher E_a was observed for coarse and moderately coarse powders in the nitrogen atmosphere, and no influence was observed on E_a for the particle sizes in the synthetic air atmosphere. The samples showed activity against the studied bacteria, and an increase in antimicrobial activity occurred with the reduction in particle size. Differences in particle sizes can influence the quality, safety, and efficacy of herbal medicines, and thermal analysis can be used to control the quality of these products.

References

1. Gavamukulya Y, Wamunyokoli F, El-Shemy HA. Annona muricata: is the natural therapy to most disease conditions including cancer growing in our backyard? A systematic review of its research history and future prospects. Asian Pac J Trop Med. 2017;10:835–48.

2. Gavamukulya Y, Abou-Elella F, Wamunyokoli F, et al. Phytochemical screening, anti-oxidant activity and in vitro anticancer potential of ethanolic and water leaves extracts of *Annona muricata* (Graviola). Asian Pac J Trop Med. 2014;7:355–63.

3. George VC, Kumar DR, Rajkumar V, et al. Quantitative assessment of the relative antineoplastic potential of the n-butanolic leaf extract of *Annona muricata* Linn. in normal and immortalized human cell lines. Asian Pac J Cancer Prev. 2012;13:699–704.

4. Bento EB, Matias EF, Brito FE Jr, et al. Association between food and drugs: antimicrobial and synergistic activity of *Annona muricata* L. Int J Food Prop. 2013;16:738–44.

5. Boyom FF, Fokou PVT, Yamthe LRT, et al. Potent antiplasmodial extracts from Cameroonian Annonaceae. J Ethnopharmacol. 2011;134:717–24.

6. Arthur FK, Larbie C, Woode E, et al. Evaluation of hepatoprotective effect of aqueous extract of *Annona muricata* (Linn.) leaf against carbon tetrachloride and acetaminophen-induced liver damage. J Nat Pharm. 2012;3:25–30.

7. Florence NT, Benoit MZ, Jonas K, et al. Antidiabetic and antioxidant effects of *Annona muricata* (Annonaceae), aqueous extract on streptozotocin-induced diabetic rats. J Ethnopharmacol. 2014;151:784–90.

8. Correa J, Ortiz D, Larrahondo J, Sanchez M, et al. Actividad antioxidante en guanábana (*Annona muricata* l.): una revisión bibliográfica. Bol Latinoam Caribe Plantas Med Aromát. 2012;11:111–26.

9. Nawwar M, Ayoub N, Hussein S, et al. Flavonol triglycoside and investigation of the antioxidant and cell stimulating activities of *Annona muricata* Linn. Arch Pharmacal Res. 2012;35:761–7.

10. Moghadamtousi SZ, Fadaeinasab M, Nikzad S, et al. *Annona muricata* (Annonaceae): a review of its traditional uses, isolated acetogenins and biological activities. Int J Mol Sci. 2015;16:15625–58.

11. Coria-Tellez AV, Montalvo-Gónzalez E, Yahia EM, et al. *Annona muricata*: a comprehensive review on its traditional medicinal uses, phytochemicals, pharmacological activities, mechanisms of action and toxicity. Arab J Chem. 2016;11:662–91.

12. Wahab A, Mariam S, Jantan I, Haque M, Arshad L. Exploring the leaves of *Annona muricata* L. as a source of potential anti-inflammatory and anticancer agents. Front Pharmacol. 2018;9:661. https://doi.org/10.3389/fphar.2018.00661.

13. Quílez AM, Fernández-Arche MA, García-Giménez MD, De la Puerta R. Potential therapeutic applications of the genus Annona Local and traditional uses and pharmacology. J Ethnopharmacol. 2018;25:244–70.

14. Yuan SSF, Chang HL, Chen HW, Yeh YT, Kao YH, Lin KH, Su JH. Annonacin, a mono-tetrahydrofuran acetogenin, arrests cancer cells at the G1 phase and causes cytotoxicity in a Bax-and caspase-3-related pathway. Life Sci. 2003;72(25):2853–61. https://doi.org/10.1016/S0024-3205(03)00190-5.

15. Correia LP, Procópio JVV, Santana CP, et al. Herbal medicine physical quality evaluation by thermal analysis using adapted Ozawa method. J Therm Anal Calorim. 2015;122:207–14. https://doi.org/10.1007/s10973-015-4638-5.

16. Cardoso IC, Pereira HMG, Tappin MRR, et al. Influência da técnica de extração e do tamanho de partícula do material vegetal no teor de compostos fenólicos totais da tintura das folhas de Alpinia zerumbet. Rev Fitos. 2017;11:62–8.

17. Correia LP, Procópio JVV, de Santana CP, et al. Characterization of herbal medicine with different particle sizes using pyrolysis GC/MS, SEM, and thermal techniques. J Therm Anal Calorim. 2013;111:1691–8. https://doi.org/10.1007/s10973-011-2129-x.

18. Santana CP, Medeiros FD, Correia LP, Diniz PHGD, Véras G, Medeiros ACD. Dissolution and uniformity of content of tablets developed with extract of *Ximenia americana* L. PLoS ONE. 2018;13(5):e0197323. https://doi.org/10.1371/journal.pone.0197323.

19. Ekere KE, Isimi YC, Okoh JE, Olobayo KO, Emeje MO. Differential scanning calorimetry and thin layer chromatography: emerging tools for predicting stability of herbal products. J Herb Med. 2017;9:74–80.

20. de Lima Ramos Júnior FJ, da Silva KMA, Brandão DO, et al. Investigation of the thermal behavior of inclusion complexes with antifungal activity. J Therm Anal Calorim. 2018;133:641–8. https://doi.org/10.1007/s10973-018-7040-2.

21. Lavor EP, Navarro MVM, Freire FD, et al. Application of thermal analysis to the study of antituberculosis drugs–excipient compatibility. J Therm Anal Calorim. 2014;115:2303–9. https://doi.org/10.1007/s10973-013-3050-2.

22. Galvão FP, De Brito WA, Dantas MG, et al. Thermal characterization of some guanylhydrazones by thermal and nonthermal techniques. J Therm Anal Calorim. 2015;120:879–87. https://doi.org/10.1007/s10973-014-4332-z.

23. Chaves TP, Fernandes FHA, Santana CP, et al. Evaluation of the interaction between the *Poincianella pyramidalis* (Tul.) LP Queiroz extract and antimicrobials using biological and analytical models. PloS One. 2016;11:1–23. https://doi.org/10.1371/journal.pone.0155532.

24. Correia LP, de Santana CP, da Silva KMA, et al. Physical and chemical characteristics of *Maytenus rigida* in different particle sizes using SEM/EDS, TG/DTA and pyrolysis GC–MS. J Therm Anal Calorim. 2018;131:743–52. https://doi.org/10.1007/s10973-016-5999-0.

25. Correia LP, Santana CP, Medeiros ACD, et al. Sideroxylon obtusifolium herbal medicine characterization using pyrolysis GC/MS, SEM and different thermoanalytical techniques. J Therm Anal Calorim. 2016;123:993–1001. https://doi.org/10.1007/s10973-015-4986-1.

26. Guimarães GP, Santos RL, Brandão DO, et al. Thermoanalytical characterization of herbal drugs from *Poincianella pyramidalis* in different particle sizes. J Therm Anal Calorim. 2018;131:661–70. https://doi.org/10.1007/s10973-016-6076-4.

27. Cuinica LG, Macêdo RO. Thermoanalytical characterization of plant drug and extract of *Urtica dioica* L. and kinetic parameters analysis. J Therm Anal Calorim. 2018;133:591–602. https://doi.org/10.1007/s10973-018-6986-4.

28. Smith RE, Tran K, Richards KM. Bioactive annonaceous acetogenins. In: ur Rahman A, editor. Studies in natural products chemistry, vol. 41. Amsterdam: Elsevier; 2014. p. 95–117. https://doi.org/10.1016/B978-0-444-63294-4.00004-8.

29. Brandão DO, Guimarães GP, Santos RL, et al. Model analytical development for physical, chemical, and biological characterization of *Momordica charantia* vegetable drug. J Anal Methods Chem. 2016;2016:1–15. https://doi.org/10.1155/2016/7528297.

30. Fernandes FHA, Boylan F, Salgado HRN. Quality standardization of herbal medicines of *Spondias dulcis* Parkinson using analytical and microbiological analysis. J Therm Anal Calorim. 2018. https://doi.org/10.1007/s10973-018-7486-2.

31. da Costa RS, Negrão CAB, Camelo SRP, et al. Investigation of thermal behavior of *Heliotropiumindicum* L. lyophilized extract by TG and DSC. J Therm Anal Calorim. 2013;111:1959–64. https://doi.org/10.1007/s10973-011-2088-2.

32. Radji M, Kurniati M, Kiranasari A. Comparative antimycobacterial activity of some Indonesian medicinal plants against multidrug resistant *Mycobacterium tuberculosis*. J Appl Pharm Sci. 2015;5:19–22.

33. Van de Venter M, Pruissen M, Koekemoer T. In vitro anti-HIV and-TB activities of *Annona muricata* and *Artemisia afra* extracts. Planta Med. 2014;80:1–29.

34. Valle AC, Gabas G, Gabriel N, et al. Ethanol extract of plants from biome'cerrado'active against bacteria related to respiratory disease in pets. Planta Med. 2014;80:1–15.

35. Takahashi JA, Pereira CR, Pimenta LP, et al. Antibacterial activity of eight Brazilian Annonaceae plants. Nat Prod Res. 2006;20:21–6.

36. Kostova I, Dinchev D. Saponins in Tribulus terrestris—chemistry and bioactivity. Phytochem Rev. 2005;4:111–37.

37. Viera GHF, Mourão JA, Ângelo ÂM, et al. Antibacterial effect (in vitro) of *Moringa oleifera* and *Annona muricata* against Gram positive and Gram negative bacteria. Rev Inst Med Trop São Paulo. 2010;52:129–32.